

Abstract

Long distance optical communication systems experience a large degree of attenuation due to fibre losses, necessitating signal amplification. Erbium Doped Fibre Amplifiers (EDFAs) have found widespread use as all-fibre optical amplifiers, but exhibit unequal amplification of different wavelengths. Since the gain spectrum is signal-power and pump-power dependent, each EDFA spectrum may differ considerably, and a tuneable gain equalizer is required. A tuneable long-period grating (LPG) can be implemented as a gain equalizer for EDFAs.

This dissertation deals with the design of an integrated optic version of the tuneable equalizing filter. The various components of which the device comprises, including optical couplers, Mach-Zehnder interferometers and an LPG, are investigated. The integrated optics designs of these components are then done using the BeamPROP software package. The use and optical properties of germania-doped silica as photosensitive waveguide material is studied. The production of the films for the gain equalizer, using electron-cyclotron resonance plasma-enhanced chemical vapour deposition, is discussed. Characterization of these films was carried out using spectroscopic ellipsometry and infrared spectroscopy. The optical constants, thickness, germania content and hydroxyl absorption was calculated using these measurements.

Contents

1 Introduction	7
1.1 Background	8
1.2 Objectives of the investigation	9
1.3 Layout of the investigation	9
2 Erbium Doped Fibre Amplifiers	13
2.1 Principle of operation	14
2.1.1 Energy levels and lifetimes	14
2.1.2 EDFA configurations and pump wavelengths	15
2.1.3 Influence of Er^{3+} -ion concentration	17
2.1.4 Advantages	18
2.2 Modelling EDFAs	18
2.3 Gain equalizing schemes for EDFAs	20
2.4 The tuneable LPG gain equalizer	24

2.4.1	Experimental setup of the tuneable LPG	24
2.4.2	Theoretical transfer function of the tuneable LPG	24
2.4.3	Experimental implementation of the tuneable LPG	26
2.4.4	The Mach-Zehnder interferometer	28
2.5	Conclusion	29
3	Integrated-optic tuneable gain equalizer	35
3.1	Optical properties of $GeO_2 : SiO_2$	36
3.1.1	Propagation loss and bending radius	39
3.2	Long-period gratings	40
3.2.1	Introduction	40
3.2.2	Principle of operation	42
3.2.3	Simulation of an LPG	43
3.3	Optical couplers	47
3.3.1	Tuneable couplers	50
3.4	Designs using BeamPROP software	52
3.4.1	The beam propagation method	52
3.4.2	Simulation setup	54
3.4.3	3-dB directional coupler design	57
3.4.4	Tuneable MZI coupler design	60
3.4.5	Long-period grating design	62
3.5	Conclusion	64

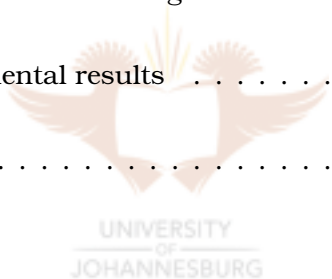
4 Deposition of GeO_2-doped SiO_2 films	69
4.1 ECR- PECVD	70
4.1.1 Chemical Vapour Deposition	70
4.1.2 Plasma processes	71
4.1.2.1 Sheath formation[2]	75
4.1.2.2 Pressure	76
4.1.2.3 Electron Cyclotron Resonance	77
4.1.2.4 Advantages of ECR-PECVD	78
4.1.2.5 RF biasing of the substrate	79
4.2 Domex MDECR-PECVD	80
4.2.1 The gas distribution system	80
4.2.2 The reactor chamber, microwave antennas and ECR magnets	81
4.2.3 The pumping station	84
4.2.3.1 The turbo molecular pump[8, 9]	84
4.2.3.2 The rotary vane pump	85
4.2.4 Pressure Gauges	86
4.2.4.1 Pirani gauges	86
4.2.4.2 Capacitance manometer	87
4.2.4.3 Penning gauges	89

CONTENTS vii

4.3	The use of $GeO_2 : SiO_2$ waveguides	90
4.3.1	Photosensitivity	90
4.3.2	Optical waveguide fabrication and structure	92
4.4	Description of the fabrication process	94
4.4.1	Depositions done at the COCS	95
4.4.2	Deposition of $a - C : H$	95
4.4.3	Deposition of SiO_2	96
4.4.4	Deposition of $GeO_2 : SiO_2$	97
4.4.5	Etching of the reactor	98
4.5	Conclusion	99
5	Ellipsometry	103
5.1	Fundamentals of ellipsometry	104
5.1.1	Electromagnetic formalism	107
5.2	Single wavelength ellipsometers	109
5.3	Spectroscopic ellipsometers	111
5.4	Modelling of ellipsometric data	113
5.4.1	Use of the DeltaPsi II software	113
5.4.2	Modelling of manufactured samples	118
5.4.2.1	Deposition of $a - C : H$	119
5.4.2.2	Deposition of SiO_2	119
5.5	Conclusion	121



<i>CONTENTS</i>	viii
6 Results	125
6.1 Characterization of the photosensitive films	126
6.2 GeO_2 content	130
6.3 Transmission spectroscopy	133
6.4 Conclusion	138
7 Conclusion and future work	141
7.1 Conclusion	142
7.1.1 Simulations and design	142
7.1.2 Experimental results	142
7.2 Future work	143



List of Figures

2.1	Erbium energy level diagram and stimulated emission . . .	14
2.2	Example of an EDFA	16
2.3	EDFA pumping schemes: (a) co-directional pumping (b) counter-directional pumping and (c) dual pumping. WSC: wavelength selective coupler.	17
2.4	EDFA gain spectrum	20
2.5	Tuneable MZI gain equalizer	23
2.6	Tuneable LPG gain equalizing filter	24
2.7	Example transmission spectrum of an LPG	25
2.8	Transmission spectrum of the TEF	26
2.9	Experimental determined relative attenuation spectra[8]	27
2.10	EDFA and flattened gain spectrum[8]	27
3.1	Illustration of the effective index method	37
3.2	Grating period calculation for various cladding modes	41

<i>LIST OF FIGURES</i>	2
3.3 Operation of an LPG	43
3.4 Normalized frequency V versus ηd	46
3.5 Transmission of an LPG	47
3.6 Symmetrical four-port coupler	48
3.7 Power transfer with increased coupling length	49
3.8 An array of lenses equivalent to the beam-shape transformation expressed by the BPM.	53
3.9 Simulation of the fundamental mode in the XY-plane	56
3.10 Three dimensional view of the fundamental mode	56
3.11 Designed 3-dB directional coupler	57
3.12 Simulation results for 3-dB directional coupler	58
3.13 2×1 MMI coupler	59
3.14 Designed tuneable MZI coupler	60
3.15 Simulation results for tuneable MZI coupler	61
3.16 Influence of temperature on the coupling ratio	62
3.17 Designed long-period grating	63
3.18 Simulation results for long-period grating	63
4.1 Generic CVD system	71
4.2 ECR Phenomenon[1]	78

<i>LIST OF FIGURES</i>	3
4.3 Domex MDECR-PECVD system	80
4.4 Schematic of DomeX MDECR-PECVD reactor chamber . .	82
4.5 Plasma source	82
4.6 Impedance matching unit	83
4.7 Matrix distribution of the ECR microwave antennas	83
4.8 Etching and deposition plasmas	84
4.9 Rotor and stator discs of turbo molecular pump.	85
4.10 Rotary vane pump.	86
4.11 Pirani Gauge.	87
4.12 Capacitance manometer	88
4.13 Penning Gauge	89
4.14 Fabrication process of a buried channel waveguide	93
4.15 Schematic of INFRASIL substrate and GeO_2 -doped SiO_2 film	94
5.1 Δ and Ψ vs angle of incidence	105
5.2 Reflection of light on a surface	107
5.3 Reflection of light from a film on a substrate	108
5.4 The AutoEL-II Ellipsometer configuration	110
5.5 The Phase Modulation Ellipsometer	112

5.6 Model of SiO_2	113
5.7 Simulated model and acquired data	114
5.8 Dispersion of SiO_2	115
5.9 Model fitted to acquired data	116
5.10 User defined (classical Lorentz oscillator) dispersion for SiO_2	116
5.11 Comparison between two films of different thickness	117
5.12 SiO_2 layer grown by point injection	120
5.13 SiO_2 layer grown by volume injection	120
6.1 Change in refractive index with increased GeH_4 flow at 1550 nm	126
6.2 Refractive index vs wavelength for different GeH_4 flow rates	127
6.3 Calculated thickness at 1.5 cm spaced positions on the wafers	128
6.4 Refractive index at 2 eV at 1.5 cm spaced positions on the wafers	129
6.5 Dispersion relations using Sellmeier equations[1]	131
6.6 Relation between theoretical refractive index and molar percentage GeO_2	131
6.7 Germane flow versus molar percentage GeO_2	132
6.8 Refractive index versus germane flux	132
6.9 Transmission spectra of Infrasil substrate	134

<i>LIST OF FIGURES</i>	5
6.10 Transmission spectra of film T1	135
6.11 Transmission spectra of film T2	135
6.12 Transmission spectra of film T3	136
6.13 Hydroxyl absorption for T1, T2 and T3	137



List of Tables

2.1 Summary of gain flattening methods[9]	21
4.1 Surface reactions[2]	73
4.2 SiO_2 and SiO_xN_y deposition	95
4.3 Reactor conditions during SiO_2 deposition	96
4.4 $Ge : SiO_2$ Depositions	97
4.5 Deposition information for samples T1, T2 and T3	98
5.1 SiO_2 and SiO_xN_y refractive indices and thicknesses	118
5.2 SiO_2 Growth rate	119
6.1 $GeO_2 : SiO_2$ layers	126
6.2 Deposition information for samples T1, T2 and T3	129
6.3 Estimated refractive indices at 1550 nm	129
6.4 Sellmeier parameters	130
6.5 Calculated molar percentage GeO_2 using Sellmeier equation and rule of mixtures	133